RSC Advances

PAPER

View Article Online
View Journal | View Issue

Cite this: *RSC Adv.*, 2017, **7**, 5189

Infrared thermochromic properties of monoclinic VO_2 nanopowders using a malic acid-assisted hydrothermal method for adaptive camouflage

Haining Ji, Dongqing Liu,* Haifeng Cheng, Chaoyang Zhang, Lixiang Yang and Dewei Ren

Received 13th November 2016
Accepted 4th January 2017

DOI: 10.1039/c6ra26731a

www.rsc.org/advances

Monoclinic VO_2 nanopowders were synthesized using a malic acid-assisted hydrothermal method. The derived VO_2 nanopowders were characterized by X-ray diffraction, Fourier transform infrared spectroscopy, Raman spectroscopy and scanning electron microscopy. The phase transition properties of the monoclinic VO_2 nanopowders were studied using differential scanning calorimetry, which displayed an obvious phase transition at 67.2 °C with a narrow thermal hysteresis width of 4.9 °C. Also, the resistance–temperature relationship and the thermal infrared images in the waveband 7.5–13 μm were analyzed. The results showed that the VO_2 samples have excellent electrical properties with resistance changes as large as two orders of magnitude. The VO_2 nanopowders obtained can control their infrared radiation intensity actively and lower their radiation temperature. Furthermore, the stability of the VO_2 nanopowders was investigated. The results showed that the VO_2 nanopowders have good thermal stability, oxidation resistance below 375 °C in an air atmosphere and humidity resistance, which has great application prospects in adaptive infrared camouflage technology.

1 Introduction

With the rapid development of modern technology, military reconnaissance and precision guided technology is widely used. Target survivability on the battlefield is also facing a great threat, so it is important to develop camouflage and stealth technology for modern warfare.[1] Traditional camouflage is achieved by wearing a camouflage coat with similar colors or textures to the surroundings, which is only used to camouflage military objectives in a fixed background.[2] However, as the location changes, these may be discovered by enemies because of the differences between the camouflage coat and the new background. Adaptive camouflage technologies are being developed. The target is to make military armed forces more mobile and better protected. Ideally, adaptive camouflage could exhibit active changes to the object's surroundings by varying its color and infrared characteristics, acting as perfect concealment from visual and infrared detection.[3]

Vanadium dioxide (VO_2) has intrigued researchers for almost six decades since Morin first discovered its temperature-driven metal-insulator transition ($T_c \approx 68$ °C).[4] Accompanied with the phase transition, VO_2 shows a reversible abrupt change in resistivity and infrared emissivity.[5–7] These promising properties make VO_2 an ideal key material in adaptive infrared camouflage.

So far, the study on adaptive infrared camouflage of VO_2 mainly focuses on thin films.[8–12] Among them, Mikhail A. Kats *et al.*[10] reported that VO_2 films showed large broadband negative differential thermal emittance property and could be used in infrared camouflage. Based on this, Xiao Lin *et al.*[11] also reported a VO_2/graphene/CNT (VGC) sandwich-like structure adaptive thermal camouflage artificial system, which can blend into the surrounding background by electric heating to cheat thermal imaging cameras. Recently, our group has also prepared VO_2 thin films and W doped VO_2 thin films, which can control its emissivity and infrared radiation intensity actively and lower its radiation temperature.[8,12] Compared with thin films, VO_2 nanopowders are better suitable for the surface of substrates with a large surface area and/or complex morphology due to both technical and cost problems.[13,14] And VO_2 nanopowders can remarkably lessen the stress for the phase changes and have broader application.[14] Therefore, it is urgent to study the infrared camouflage properties of the VO_2 nanopowders.

In this paper, monoclinic VO_2 (VO_2 (M)) nanopowders were synthesized *via* a novel one-step hydrothermal method with an ideal environmental friendly reducing agent malic acid. Thermal infrared images of VO_2 (M) nanopowders were tested under different temperature based on thermal imaging camera working in the waveband 7.5–13 μm. And it was found that the VO_2 (M) nanopowders obtained can control its infrared radiation intensity and lower its radiation temperature. Finally, the stability of VO_2 (M) nanopowders was studied for further development of the application.

Science and Technology on Advanced Ceramic Fibers and Composites Laboratory, National University of Defense Technology, Changsha 410073, P. R. China. E-mail: dongqingliu@ymail.com; Tel: +86 0731 84576440

2 Experimental

All reagents were purchased from Aladdin chemical reagent corporation and used without further purification. VO_2 (M) nanopowders were prepared by a novel one-step hydrothermal method using a vanadium source of ammonium metavanadate (NH_4VO_3) and a reducing agent of malic acid ($C_4H_6O_5$) without additional surfactant. In a typical synthesis, 2.34 g NH_4VO_3 and 4.02 g $C_4H_6O_5$ were dispersed in 60 mL deionized water. The mixture was stirred for 30 min and then transferred to a 100 mL Teflon-lined stainless-steel autoclave. The hydrothermal reaction was carried out at 260 °C for 24 h and then air-cooled to room temperature. The final products were collected *via* centrifugation, washed with deionized water and ethanol three times and dried in a vacuum drying oven at 80 °C for 12 h.

The crystalline structure of VO_2 (M) nanopowders was characterized by a Bruker D8 advance diffractometer equipped with monochromatic Cu Kα radiation ($\lambda = 0.15406$ nm). The composition of the nanopowders were characterized *via* a Bruker Vertex 70 Fourier transform infrared spectroscopy (FTIR) instrument using KBr pellet method and a Horiba JY HR Evolution Raman Spectroscopy with excitation wavelength 532 nm. The morphology was obtained using a NOVA NanoSEM 230 field-emission scanning electron microscope (FESEM). The phase transition behaviors of the nanopowders were measured by METTLER TOLEDO differential scanning calorimetry (DSC) over the temperature range from 0 to 100 °C using a liquid nitrogen cooling unit. The heating and cooling rates were set at 10 °C min^{-1}. The thermal stability of the nanopowders was studied with thermal gravimetric analysis (TGA) by TA instruments Q600 system. The temperature was increased from room temperature to 800 °C in a ramp of 5 °C min^{-1} and an air flow of 60 mL min^{-1}. The effect of humidity on the performance of the nanopowders was studied in a climate chamber which allows experiments at fixed values of temperature and humidity (RH). The treatments were performed at an ambient temperature of 25 °C and RH = 95%. The duration for the treatment was 0 h, 24 h, 48 h, 96 h, and 168 h, respectively. The samples treated were dried in a vacuum drying oven at 60 °C for 10 h in order to carry out XRD and DSC tests. The resistance measurements were performed by standard four-terminal method using a Quantum Design Physics Property Measurement System (PPMS).

In order to investigate infrared camouflage properties, thermal infrared images were tested under different temperature based on FLIR T420 thermal imaging camera operating in the waveband 7.5–13 μm. Firstly, the VO_2 (M) nanopowders need to be pressed into small rectangle pellets. Vanadium pentoxide (V_2O_5) pellets, considered as a reference, and vanadium dioxide pellets were prepared by automatic tablet press using the same operating conditions: all rectangle pellets were realized in a rectangle die kit, involving the same uniaxial pressure, and all powder samples were prepared with the same quantity. Therefore, the thickness and the surface roughness of the samples are approximately the same.

3 Results and discussion

The crystalline structure of as-prepared nanopowders were characterized by XRD. Fig. 1a showed the XRD patterns of nanopowders obtained at 260 °C for 24 h. All peaks can be indexed as a single monoclinic phase VO_2 (M) (JCPDS card. no. 43-1051). It can also be seen that all of the peaks were sharp and strong with relatively narrow peak widths, indicating the good crystallinity of VO_2 (M). The results indicated that phase-pure and well-crystallized VO_2 (M) nanopowders can be synthesized by such a novel one-step hydrothermal method. The method is very nice compared to the present ones. Firstly, for the hydrothermal synthesis, most of previously reported studies used V_2O_5 as a vanadium source,[15–17] which exhibited a toxic property, thus limited the usage and development of this method. Secondly, the preparation of VO_2 nanopowders mainly took higher-cost hydrazine as reducing agent,[18–20] which increased the cost of VO_2 nanopowders. Compared with the present method, the method with NH_4VO_3 and $C_4H_6O_5$ as starting materials has some advantages such as easy obtained raw materials, lower cost and no environmental pollution.[21,22] Especially malic acid, the reducing agent for the reaction, which can be directly obtained from apples, is an ideal environmental friendly reducing agent. This approach will aid in the large scale synthesis of pure vanadium dioxide nanopowders.

The size and morphology of typical products were illustrated using SEM images. The SEM image (Fig. 1b) and particle size distributions (Fig. 1c) of nanopowders obtained from SEM image revealed that nanopowders were sphere-like with average particle size of 91.5 nm.

To investigate the chemical bonding between vanadium and oxygen ions and to confirm the phase purity, we performed FTIR and Raman spectrum measurement. Fig. 2a showed the FTIR spectrum of VO_2 (M) samples prepared. The main vibrational bands observed from the FTIR spectrum are at 996 cm^{-1}, 715 cm^{-1}, 530 cm^{-1}, 422 cm^{-1} and can be considered as intrinsic to vanadium dioxide, which matches well with earlier reports: the initial broad vibrational band at 530 cm^{-1} and 422 cm^{-1} are assigned to the V–O–V octahedral bending modes; the band at 996 cm^{-1} and 715 cm^{-1} is attributed to the coupled vibration of V=O.[23,24] These FTIR observations confirmed that the nanopowders correspond to the VO_2 phase. Fig. 2b illustrated Raman spectrum of VO_2 (M) samples prepared. The peaks in the Raman spectrum were all identified as 141 cm^{-1}, 188 cm^{-1}, 221 cm^{-1}, 257 cm^{-1}, 304 cm^{-1}, 385 cm^{-1}, 494 cm^{-1}, and 611 cm^{-1} respectively, and these Raman-active modes were the clear evidence of the existing of VO_2 (M), which were consistent with the previous results.[25–27]

The fully reversible phase transition of the as-synthesized VO_2 (M) nanopowders are clearly revealed by DSC curves. Fig. 3(a) illustrated that the VO_2 (M) nanopowders revealed a thermal hysteresis phenomenon with a width of 4.9 °C, which was narrower than the results reported in the literature.[28,29] This may be caused by the interface effects.[30] The heating of the VO_2 (M) nanopowders was accompanied by endothermal effects at 67.2 °C in the DSC curves, corresponding to the transition

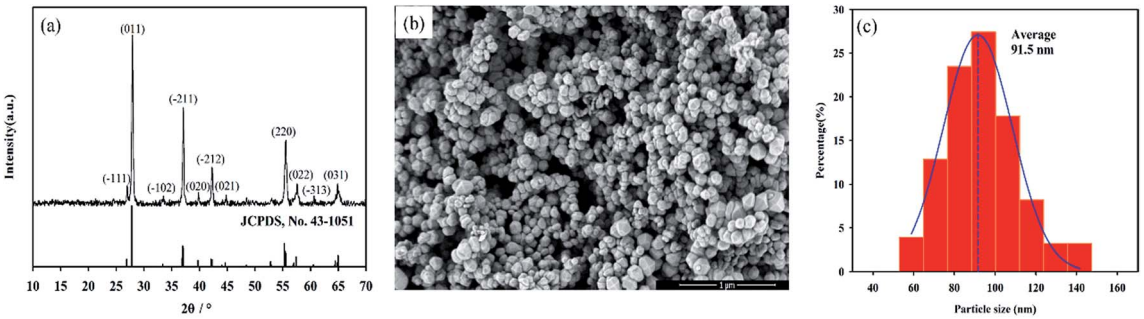

Fig. 1 XRD patterns (a), SEM images (b) and particle size distribution (c) of as-synthesized VO_2 nanopowders.

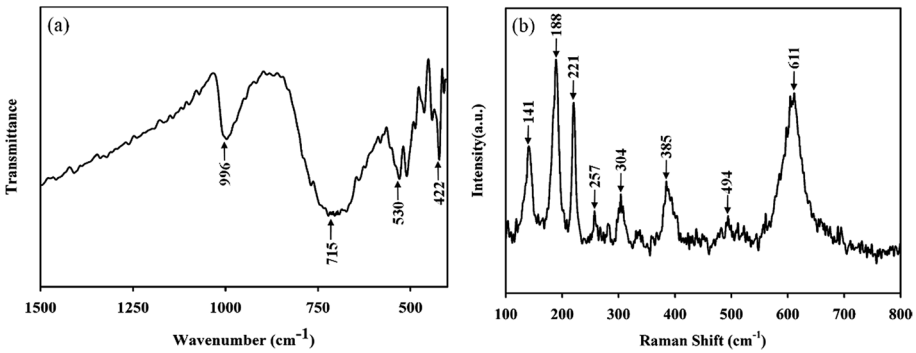

Fig. 2 FTIR spectrum (a) and Raman spectrum (b) of as-synthesized VO_2 nanopowders.

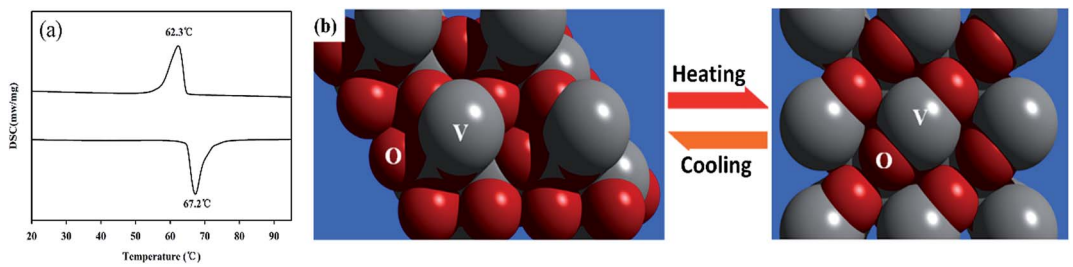

Fig. 3 (a) DSC curves of as-synthesized VO_2 nanopowder, (b) schematic of phase evolution between monoclinic VO_2 (M) and tetragonal rutile VO_2 (R).

temperature of VO_2 from the monoclinic phase VO_2 (M) to the tetragonal phase VO_2 (R) (see schematic in Fig. 3b). Accordingly, the thermal analysis results provided the direct evidence for the occurrence of temperature driven first-order phase transition in VO_2 (M) nanopowders.

As mentioned above, phase transition is one of the most critical intrinsic characteristics of VO_2 (M) which often reflected in the variation of resistance and infrared radiation. Then, to examine the thermochromic properties of VO_2 (M) nanopowders, the electrical and infrared properties were researched.

Fig. 4 showed the temperature-dependent resistance of the VO_2 (M) nanopowders in temperature range of 0–100 °C, measured in the process of both cooling and heating. It can be seen that the transition temperature of VO_2 (M) nanopowders was about 67 °C which was close to DSC results. At low temperature, VO_2 (M) exhibited an insulating state with higher resistance; but

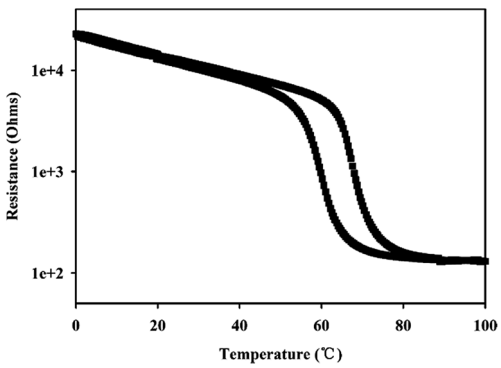

Fig. 4 Resistance *versus* temperature curve of as-synthesized VO_2 nanopowders.

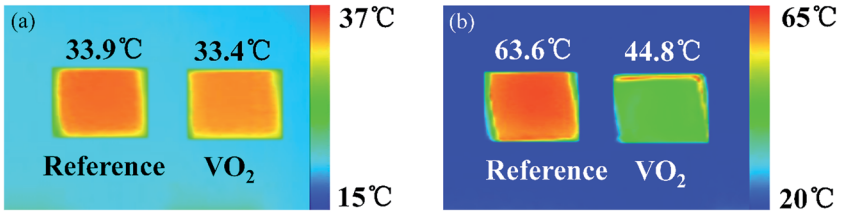

Fig. 5 The thermal infrared images of VO_2 pellets at 40 °C (a) and 75 °C (b).

they transited into metallic state when the temperature increased above the phase transition point characterized by abrupt jump of resistance. It should be noted that the resistance decreased by 2 order of magnitude as the temperature increased. The above results showed that VO_2 (M) had excellent electrical properties. The obtained VO_2 nanopowders have larger resistance jump than others' work based on thin film that resistance decreased 1.0–1.5 order of magnitude.[5,31] The abrupt and large change of the resistance indicates that the VO_2 nanopowders is stoichiometric and highly crystalline.

Thermal infrared images were characterized by thermal imaging camera to display the infrared radiation performance of VO_2 pellets. Fig. 5 showed the thermal infrared images of reference samples (V_2O_5) and VO_2 samples at different real temperature 40.0 °C and 75.0 °C. The emissivity of reference samples keep constant at the temperature 40.0 °C and 75.0 °C. During the measurement, we assured that reference samples and VO_2 samples had the same real temperature, so the difference of the radiation temperature was due to the different emissivity.

As can be seen in Fig. 5(a), when real temperature was 40 °C, radiation temperature of reference samples and VO_2 samples were 33.9 °C and 33.4 °C, respectively. There was almost no difference between the two radiation temperatures. As can be seen in Fig. 5(b), when real temperature was 75 °C, radiation temperature of reference samples and VO_2 samples were 63.6 °C and 44.8 °C, respectively, radiation temperature difference reached to 18.8 °C. The results implied that at 40 °C, VO_2 exhibited an insulating state with high emissivity and radiation intensity; but when the temperature increased to 75 °C, they transited into metallic state with low emissivity and radiation intensity. That is, thermal infrared radiation intensity of VO_2 change adaptively with outside environment change and objects will keep consistent with the outside environment persistently. Therefore, VO_2 nanopowders

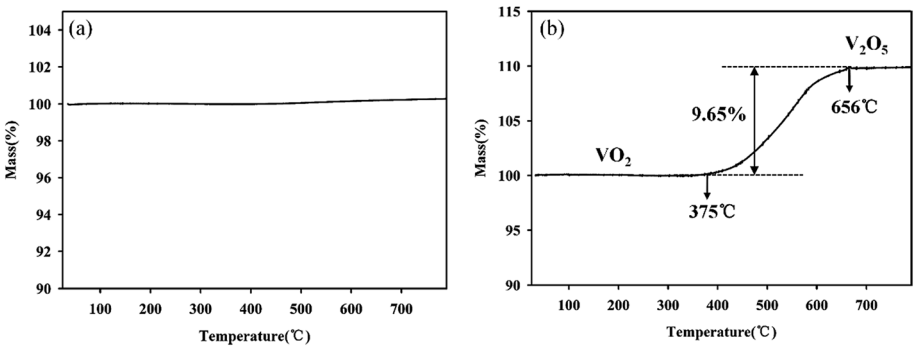

Fig. 6 TGA analyses of the as-synthesized VO_2 nanopowders in the N_2 atmosphere (a) and in the air atmosphere (b).

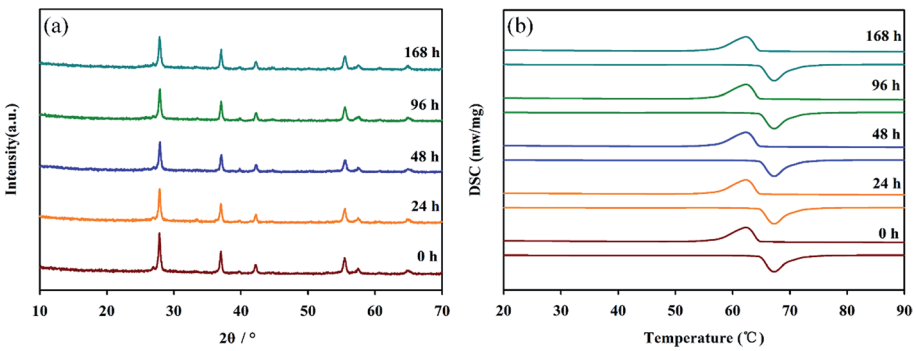

Fig. 7 XRD spectra (a) and DSC curves (b) for VO_2 nanopowders after different treatment durations at an ambient temperature of 25 °C and RH = 95%.

have great application prospects in the field of adaptive infrared camouflage technology.

For further development of the application, the stability study of the material is also very important. To understand the stability of the VO_2 (M) nanopowders, the thermal gravimetric analysis was conducted in flowing N_2 atmosphere and air atmosphere respectively, as shown in Fig. 6. As can be seen from Fig. 6a, when the powder samples were heated in the N_2 atmosphere from room temperature up to 800 °C, the quality was almost constant, indicating that it can be stable in the N_2 atmosphere. However, when the powder samples were heated in the flowing air atmosphere from room temperature up to 800 °C, the quality of powder samples increased due to oxidation by air. Fig. 6b revealed that VO_2 (M) begun to be oxidized by O_2 at 375 °C and finished at 656 °C. The weight gain is *ca.* 9.65% in its oxidative process. The weight gain values of VO_2 (M) are well corresponding to the oxidation of the bulk VO_2 to V_2O_5 (9.64%), as represented in equation: $4VO_2 + O_2 \xrightarrow{\Delta} 2V_2O_5$.

Furthermore, the effect of humidity on the performance of the nanopowders was studied. Fig. 7 showed XRD and DSC data for VO_2 nanopowders after different treatment durations at an ambient temperature of 25 °C and RH = 95%. It is clear from Fig. 7a that the crystal structure of VO_2 nanopowders did not change. And as can be seen from Fig. 7b, the positions of the exothermic peak and the endothermic peak and the enthalpy change almost did not change, which indicated that phase transition properties still retained after 168 h treatment. Based on the above results, VO_2 (M) nanopowders have good thermal stability, oxidation resistance below 375 °C in air and humidity resistance, which can be applied to adaptive infrared camouflage in air atmosphere.

4 Conclusion

In conclusion, VO_2 (M) nanopowders were successfully synthesized by a novel one-step hydrothermal method with an ideal environmental friendly reducing agent. VO_2 (M) nanopowders obtained exhibit a reversible phase transition properties with a critical temperature at 67.2 °C and a narrow hysteresis width of 4.9 °C. VO_2 (M) nanopowders obtained have excellent electrical properties with resistance changes as large as two orders of magnitude. And VO_2 (M) nanopowders obtained can control its infrared radiation intensity actively and lower its radiation temperature. Besides, VO_2 (M) nanopowders have good thermal stability, oxidation resistance below 375 °C in air atmosphere and humidity resistance, which has great application prospects in the adaptive infrared camouflage technology.

Acknowledgements

This work was supported by the Natural Natural Science Foundation of China (No. 51502344).

References

1 L. Li, X. L. Lü, B. Z. Li, X. P. Li and H. X. Wang, Evaluation of ground thermal infrared camouflage using pure technical and pure scale dynamic dea model, *Adv. Mater. Res.*, 2014, **989–994**, 2323–2327.
2 J. Zhang, J. Yu, J. F. Jiao, H. Chen and P. Liu, Preparation and properties testing of intelligent color-changing camouflage coating, *Adv. Mater. Res.*, 2013, **659**, 15–18.
3 H. Yu, S. Shao, L. Yan, H. Meng, Y. He, C. Yao, P. Xu, X. Zhang, W. Hu and W. Huang, Side-chain engineering of green color electrochromic polymer materials: toward adaptive camouflage application, *J. Mater. Chem. C*, 2016, **4**, 2269–2273.
4 F. J. Morin, Oxides which show a metal-to-insulator transition at the neel temperature, *Phys. Rev. Lett.*, 1959, **3**, 34–36.
5 F. Guinneton, L. Sauques, J. C. Valmalette, F. Cros and J. R. Gavarri, Comparative study between nanocrystalline powder and thin film of vanadium dioxide VO_2: electrical and infrared properties, *J. Phys. Chem. Solids*, 2001, **62**, 1229–1238.
6 M. E. A. Warwick and R. Binions, Advances in thermochromic vanadium dioxide films, *J. Mater. Chem. A*, 2014, **2**, 3275–3292.
7 B. Zhu, H. Tao and X. Zhao, Effect of buffer layer on thermochromic performances of VO_2 films fabricated by magnetron sputtering, *Infrared Phys. Technol.*, 2016, **75**, 22–25.
8 D. Q. Liu, H. F. Cheng, W. W. Zheng and C. Y. Zhang, Infrared thermochromic properties of VO_2 thin films prepared through aqueous sol–gel process, *J. Wuhan Univ. Technol., Mater. Sci. Ed.*, 2012, **27**, 861–865.
9 Z. P. Mao, W. Wang, Y. Liu, L. P. Zhang, H. Xu and Y. Zhong, Infrared stealth property based on semiconductor (M)-to-metallic (R) phase transition characteristics of W-doped VO_2 thin films coated on cotton fabrics, *Thin Solid Films*, 2014, **558**, 208–214.
10 M. A. Kats, R. Blanchard, S. Y. Zhang, P. Genevet, C. H. Ko, S. Ramanathan and F. Capasso, Vanadium dioxide as a natural disordered metamaterial: perfect thermal emission and large broadband negative differential thermal emittance, *Phys. Rev. X*, 2013, **3**, 041004.
11 L. Xiao, H. Ma, J. Liu, W. Zhao, Y. Jia, Q. Zhao, K. Liu, Y. Wu, Y. Wei and S. Fan, Fast adaptive thermal camouflage based on flexible VO_2/graphene/CNT thin films, *Nano Lett.*, 2015, **15**, 8365–8370.
12 D. Liu, H. Cheng, X. Xing, C. Zhang and W. Zheng, Thermochromic properties of W-doped VO_2 thin films deposited by aqueous sol–gel method for adaptive infrared stealth application, *Infrared Phys. Technol.*, 2016, **77**, 339–343.
13 Z. F. Peng, W. Jiang and H. Liu, Synthesis and electrical properties of tungsten-doped vanadium dioxide nanopowders by thermolysis, *J. Phys. Chem. C*, 2007, **111**, 1119–1122.
14 J. Li, C. Y. Liu and L. J. Mao, The character of W-doped one-dimensional VO_2 (M), *J. Solid State Chem.*, 2009, **182**, 2835–2839.
15 H. H. Yin, M. Luo, K. Yu, Y. F. Gao, R. Huang, Z. L. Zhang, M. Zeng, C. X. Cao and Z. Q. Zhu, Fabrication and

temperature-dependent field-emission properties of bundlelike VO_2 nanostructures, *ACS Appl. Mater. Interfaces*, 2011, **3**, 2057–2062.

16 W. Yu, S. Li and C. Huang, Phase evolution and crystal growth of VO_2 nanostructures under hydrothermal reactions, *RSC Adv.*, 2016, **6**, 7113–7120.

17 L. Zhang, F. Xia, Z. Song, N. A. S. Webster, J. C. Song, H. Luo and Y. Gao, Phase and morphology evolution during the solvothermal synthesis of VO_2 polymorphs, *Inorg. Chem. Front.*, 2015, **3**, 1–8.

18 Z. Gui, R. Fan, W. Q. Mo, X. H. Chen, L. Yang, S. Y. Zhang, Y. Hu, Z. Z. Wang and W. C. Fan, Precursor morphology controlled formation of rutile VO_2 nanorods and their self-assembled structure, *Chem. Mater.*, 2002, **14**, 5053–5056.

19 Z. Zhang, Y. Gao, H. Luo, L. Kang, Z. Chen, J. Du, M. Kanehira, Y. Zhang and Z. L. Wang, Solution-based fabrication of vanadium dioxide on F: SnO_2 substrates with largely enhanced thermochromism and low-emissivity for energy-saving applications, *Energy Environ. Sci.*, 2011, **4**, 4290–4297.

20 Z. Gui, R. Fan, X. H. Chen and Y. C. Wu, A new metastable phase of needle-like nanocrystalline $VO_2 \cdot H_2O$ and phase transformation, *J. Solid State Chem.*, 2001, **157**, 250–254.

21 J. Zou, Y. G. Peng and H. Lin, A low-temperature synthesis of monoclinic VO_2 in an atmosphere of air, *J. Mater. Chem. A*, 2013, **1**, 4250–4254.

22 L. Li, J. Ge, R. Chen, F. Wu, S. Chen and X. Zhang, Environmental friendly leaching reagent for cobalt and lithium recovery from spent lithium-ion batteries, *Waste Manag.*, 2010, **30**, 2615–2621.

23 I. L. Botto, M. B. Vassallo, E. J. Baran and G. Minelli, IR spectra of VO_2 and V_2O_3, *Mater. Chem. Phys.*, 1997, **50**, 267–270.

24 W. Chen, L. Mai, C. Jiang, J. Peng and Q. X. Q. Zhu, Synthesis and characterization of novel vanadium dioxide nanorods, *Solid State Commun.*, 2003, **132**, 513–516.

25 R. Chen, L. Miao, C. Liu, J. Zhou, H. Cheng, T. Asaka, Y. Iwamoto and S. Tanemura, Shape-controlled synthesis and influence of W doping and oxygen nonstoichiometry on the phase transition of VO_2, *Sci. Rep.*, 2015, **5**, 14087.

26 J. M. Wu and L. B. Liou, Room temperature photo-induced phase transitions of VO_2 nanodevices, *J. Mater. Chem.*, 2011, **21**, 5499–5504.

27 C. Cheng, K. Liu, B. Xiang, J. Suh and J. Q. Wu, Ultra-long, free-standing, single-crystalline vanadium dioxide micro/nanowires grown by simple thermal evaporation, *Appl. Phys. Lett.*, 2012, **100**, 103111.

28 Z. Song, L. Zhang, F. Xia, N. A. S. Webster, J. Song, B. Liu, H. Luo and Y. Gao, Controllable synthesis of VO_2 (D) and their conversion to VO_2 (M) nanostructures with thermochromic phase transition properties, *Inorg. Chem. Front.*, 2016, **3**, 1035–1042.

29 B. Dong, N. Shen, C. Cao, Z. Chen, H. Luo and Y. Gao, Phase and morphology evolution of VO_2 nanoparticles using a novel hydrothermal system for thermochromic applications: the growth mechanism and effect of ammonium (NH_4^+), *RSC Adv.*, 2016, 81559–81568.

30 L. Zhong, M. Li, H. Wang, Y. Luo, J. Pan and G. Li, Star-shaped VO_2 (M) nanoparticle films with high thermochromic performance, *CrystEngComm*, 2015, **17**, 5614–5619.

31 D. Zhang, K. Yang, Y. Li, Y. Liu, M. Zhu, A. Zhong, X. Cai, P. Fan and W. Lv, Employing TiO_2 buffer layer to improve VO_2 film phase transition performance and infrared solar energy modulation ability, *J. Alloys Compd.*, 2016, **684**, 719–725.

